Assembly simulation of Skin Model Shapes: a comparison of two methods taking into account external forces

X. Yan, A. Ballu

Available online at www.sciencedirect.com

ScienceDirect

Procedia CIRP 75 (2018) 303–308

www.elsevier.com/locate/procedia

15th CIRP Conference on Computer Aided Tolerancing – CIRP CAT 2018

Assembly simulation of Skin Model Shapes: a comparison of two methods taking into account external forces

X. Yan, A. Ballu*

Univ. Bordeaux, I2M, UMR 5295, 33400 Talence, France

* Corresponding author. Tel.: +33 5 56 84 5387; fax: +33 5 4000 69 64. *E-mail address:* alex.ballu@u-bordeaux.fr

Abstract

Assembly simulation of parts with form defects using Skin Model Shapes (SMS) is much more difficult than the usual assembly of ideal models in a CAD system. Some research studies try to tackle this issue, but very few authors focus on form defect, multibody system and external forces and torques, all at once. Yet external forces are preponderant when considering the relative positioning of parts with form defects.

The aim of the paper is to compare two different assembly simulation methods based on: (1) Linear Complementarity Condition (LCC), (2) elimination of contact configurations which are not in mechanical equilibrium. First, the two methods are introduced, and a theoretical comparison shows their differences. Next, several assembly cases are studied. Simulation results are compared to evaluate the proposed methods. The influences of form defect and assembly loads are emphasized through these cases.

Peer-review under responsibility of the Scientific Committee of the 15th CIRP Conference on Computer Aided Tolerancing - CIRP CAT 2018.

Keywords: Assembly simulation; Form defect; Skin Model Shape;

1. Introduction

The wide use of Information Technology (IT) facilitates tolerance management, with Computer-Aided Tolerancing (CAT) tools developed to help engineers make relevant decisions. Among these tools, the Offset Zone-based method [1] is introduced to represent the geometry of tolerance zones. The Technologically and Topologically Related Surfaces (TTRS) model [2] is developed to construct datum systems. Small Displacement Torsor (SDT) is used to evaluate and represent manufacturing defects [3]. Models such as Vectorial tolerancing model [4], Jacobian-Torsor model [5] Proportioned Assembly Clearance Volume (PACV) [6] and Tolerance Map (T-Map®) [7] are proposed to calculate the ranges of assembly deviation. The above-mentioned tolerance analysis methods use ideal features, which contain no form defects. To emphasize the influence of form defects and cover different precision levels of manufacturing defects, the concept of the skin model is proposed by Ballu and Mathieu [8]. The skin model shape, the discrete instance of the skin model, is used to simulate manufacturing defects [9] and conduct tolerance analysis [10–14].

This article investigates optimization-based methods to simulate skin model shape assembly. The relation between assembly boundary condition and optimization objective is analyzed. Based on the analysis, two simulation methods are proposed. The principle behind the methods and their simulation results are compared.

2. Analysis of Assembly Considering Form Defects and Assembly Loads

Considering form defects during assembly imposes many more difficulties than when they are not taken into consideration. The first step consists in investigating the assembly configurations which are due to form defects. In this section, the simulation models, assembly conditions and final assembly configurations are studied. The study highlights the important elements and provides guidelines for developing simulation methods.

2212-8271
Peer-review under responsibility of the Scientific Committee of the 15th CIRP Conference on Computer Aided Tolerancing - CIRP CAT 2018.
10.1016/j.procir.2018.04.072

To start from basic cases, we look at the mating of two parts with planar contact surfaces. Fig. 1 shows the assembly, and the red arrow indicates the assembly force. The nominal model should be perfectly mated, as can be seen in Fig. 1(a).

The ideal surface-based deviation model contains translation and rotation deviations, while the mating planes are still ideal plane features. This means the planes could be expressed by a center point and a normal vector. Using normal vectors, the orientation of two parts after assembly could be determined. As in nominal models, the two planes can still mate without gaps, as can be seen from Fig. 1(b). Here, considering static friction forces, displacements according to the DOFs are zero.

Thus in the configuration shown in Fig. 1(b), without friction, the top part would slide to the left because the planar surface is not normal to the force. As there is a degree of freedom, the tangential displacement is constrained. This constraint replaces the friction force. The concept of support, used in FEA, will be used in the following part of the paper to put these constraints in place.

The problem becomes difficult when considering skin model shapes in Fig. 1(c). Since form defects are being considered, the two mating surfaces are no longer ideal plane features. The mating of two surfaces is also reduced to certain contact regions only. The resulting assembly depends on the local contacts between the two surfaces, and the local contacts depend on:

- The form defects on mating surfaces.
- The position and direction of assembly forces.

As in the configuration in Fig. 1(c), there could be tangential displacements due to local contacts which are not normal to the force. Thus, the tangential displacements are also constrained to zero.

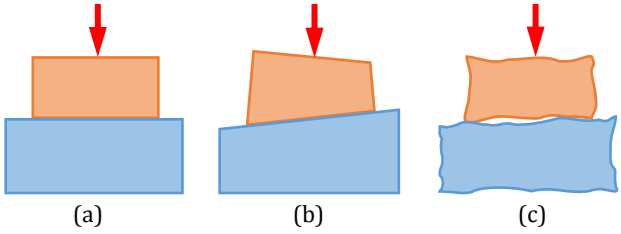

Fig. 1. Mating of two parts with two plane surfaces: (a) nominal models (b) polyhedral deviation models (c) skin model shapes.

For a better understanding, a close view of the mating surfaces is shown in Fig. 2. The two lines in different colors represent two mating surfaces in 2D. In Fig. 2(a), the assembly force is applied close to the center of the surface, and one mating configuration is found. When moving the assembly force to the left side of the surface, the contact regions also shift. The shifting of contact regions is determined by the form defects and assembly force at the same time. This indicates that when we are considering form defects in assembly, we should also consider assembly loads.

The assembly simulation could be considered as the relative positioning of skin model shapes. In the following, details about contact and force during assembly simulation are discussed.

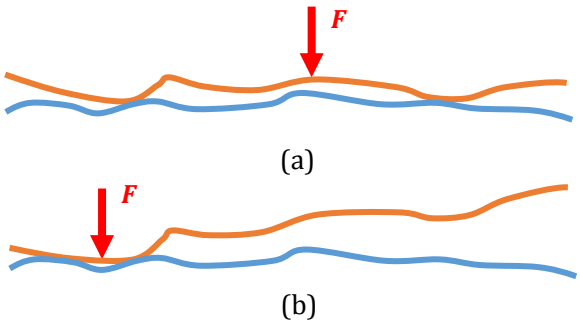

Fig. 2. Influences of form defects and force:
(a) force applied to center point (b) force applied close to left side.

2.1. Discrete Representation of Skin Model Shapes

Based on the discrete description of skin model shapes [9], we chose to use point clouds to represent features with form defects in 2D. As shown in Fig. 3, section views of two mating planes $SF1$ and $SF2$ are constructed by discrete points. $N1$ and $N2$ are the normal direction of corresponding nominal planes (dashed lines in the figure), and we assume the points have the same normal direction as the nominal planes. During the relative positioning process, $SF1$ is the target part (fixed) and $SF2$ is the object part which moves to mate with $SF1$.

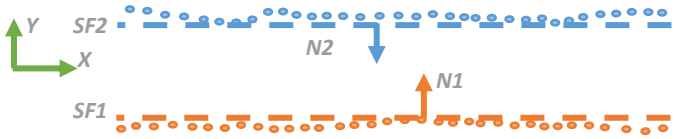

Fig. 3. Two planes expressed by point clouds.

2.2. Signed Distance and Non-penetration Constraint

The sign is defined to indicate the relative direction, the envelope condition or the material condition. For example, as shown in Fig. 4(a), the distance between $P1$, $P2$ and the discrete circle are evaluated. To identify that the point is inside or outside the circle, a signed distance could be used. Let $P1$ be a point outside the circle, it has a positive distance, and let $P2$ be a point inside the circle, it has a negative distance. Similarly for material, let us consider that a point inside the material has a negative distance and a point outside the material has a positive distance. Fig. 4(b) shows the example of material distance, where the hatching indicates the material and the points form the part surface. In this case, $P2$ has negative material distance to the surface while $P1$ has positive material distance.

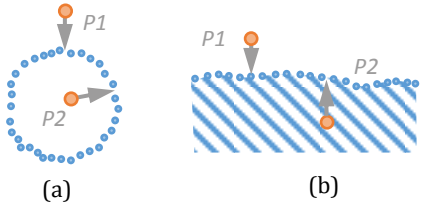

Fig. 4. Examples of signed distances.

Using signed distances, we can set linear constraints, in Fig. 3, for example. Let P_{SF1} and P_{SF2} be two points on planes $SF1$ and $SF2$. The signed distance is defined as D_{sign} in Equation (*1*). In assembly, the signed distance between mating surfaces is constrained to be non-negative to express that there is no penetration.

$$D_{sign} = P_{SF1}P_{SF2} \cdot N1 = P_{SF2}P_{SF1} \cdot N2 \quad (1)$$

2.3. Constraints on Degree of Freedom (DOF)

The concept of SDT (Small Displacement Torsor) was developed by Bourdet and Clément [3,15] to fit geometrical surfaces to point clouds. Based on the kinematics of a rigid body in Euclidean space, the displacement of the part could be described by a torsor that contains 3 translations and 3 rotations. In applying this to metrology and tolerancing, the displacements are assumed to be small and can be linearized by torsor. Equation (*2*) shows the SDT of a rigid part A, identified by rotations α, β, γ and translations u, v, w. Using SDT, the relation between displacement and geometric characteristics (like distance and angle) can also be linearized.

$$\{d\}_A = \{\vec{R} \quad \vec{T}\}_A = \begin{Bmatrix} \alpha & u \\ \beta & v \\ \gamma & w \end{Bmatrix}_A \quad (2)$$

During the relative positioning of skin model shapes, not all of the 6 torsor variables are free. For the example in Fig. 3, the displacement of $SF2$ along direction x will cause infinite solutions. In addition, in the physical assembly of parts, due to static friction, there will be no translation along direction x. Therefore the DOF of $SF2$ along direction x should be fixed. Moreover, for complex assembly, the constraints on DOFs should be analyzed to guarantee that the problem could be solved.

2.4. Load Boundary Conditions

In the work of Samper et al. [10], the distance between two planar surfaces is minimized in consideration of the assembly force. Homri et al. [14] and Ledoux et al. [16] extended this method to cylindrical and spherical joints, respectively. The difficulty is in generalizing this method to more complex assemblies. Similarly, the method developed by Corrado et al. [12] is not extended to general cases. In the work of Schleich et al. [11], efforts were made to generalize the problem by assigning weights to get a multi-objective optimization problem. However, selecting the weights is no trivial matter, and there are no clues on how to define them.

There are several ways to take into account the influence of assembly loads. One method is to transform it into an optimization objective, such as maximization of the displacement along the load direction:

$$objective: max(disp) \quad (3)$$

where $disp$ is the displacement of the skin model shape along the load direction. Another choice is to integrate load boundary conditions into optimization constraints.

2.5. Simplification of Assembly Loads

For general cases, several assembly loads may be applied to the skin model shapes. A method to simplify the loads is therefore introduced.

The method is based on Poinsot's theorem [17] from the torsor theory (also called screw theory). According to the theorem any forces or torques applied to one system could be simplified to one force applied at a certain point in the space and one torque applied along the same direction.

Using this theorem, we can reduce multiple forces and torques to only one force and one torque.

3. Displacement Maximization Method

To simulate the assembly of rigid parts, there are several solutions. Using simulation methods from the field of robotics or multibody dynamics, the whole assembly process could be simulated. For tolerance analysis, however, the precision of the final assembly plays a critical role while the dynamic properties are not concerned. Moreover, to be able to conduct a statistical simulation, the calculation time should be reduced. For these two reasons, the dynamic methods are not suitable for our problem. In this section a Displacement Maximization (DM) based method is proposed to meet these demands.

3.1. Formulation of the Problem

In the DM method, the objective is to maximize the displacement of the skin model shape along the load direction. This displacement is represented by $disp$ in Equation (*4*):

$$\begin{aligned} find \quad & X = [SDTs] \\ max \quad & (disp) \\ s.t. \quad & D_{sign} \geq 0 \end{aligned} \quad (4)$$

where $SDTs$ are small displacement torsors of skin model shapes. $D_{sign} \geq 0$ indicates that there is no penetration between models. The optimization problem could be solved efficiently by linear programming algorithms, such as simplex.

3.2. Optimization Constraints and Objective

The constraints and objectives should be adjusted according to the detailed simulation cases. For example, additional constraints on DOFs can be introduced to simplify the assembly model. Suitable displacement constraints guarantee the solvability and efficiency of the optimization resolution. Therefore, they should be defined carefully.

Based on assembly load boundary condition analysis, we define the optimization objective according to the following steps:

a) Define a point on the object part where the load is applied;
b) Define a vector, its direction is the load direction of the force, or is parallel to the rotation axis of torque load;
c) The objective is to maximize the displacement of the object part along/around the vector direction defined in step b).

Using this method, a link between optimization objective and assembly boundary conditions is established.

The load boundary condition could contain force and torque at the same time. In this case, two optimization objectives are defined, and the optimization is conducted using these two objectives alternatively. Depending on the order in which the two objectives are applied, there will be two simulation results.

For the assembly of multiple skin model shapes, the sequence of positioning influences the simulation result. Optimization objectives corresponding to each sequence can be defined, and several simulation results will be generated.

Considering the mating and load conditions, not all solutions are feasible. Therefore, a balance checking process is added to select the feasible results.

3.3. Simulation Process

The DM simulation process is defined as follows:

a) Analyze and simplify load boundary conditions, define optimization objective.
b) Find displacement boundary conditions, transform them into linear constraints.
c) Conduct optimization alternatively to generate all possible assembly cases:
   - If there is more than one assembly sequence (more than one object part).
   - If the optimization objective contains translation and rotation.
d) Check the balance of the simulation result, only balanced results are accepted.

4. Linear Complementarity Condition Method

In the DM based method, the system equilibrium condition is used to select a feasible assembly configuration from several simulation results. Another strategy is to include the system equilibrium condition into the optimization directly.

In multibody dynamics contact dynamics, the Linear Complementarity Problem (LCP) is used to model the contacts between parts.[18] Inspired by the concept of Linear Complementarity Condition (LCC), this work provides such a simulation method where all assembly boundary conditions are considered together.

4.1. Principle of LCC

The principle of LCC is explained by Fig. 5. For two surfaces S_1 and S_2, and their contact points A_1 and A_2, there are two configurations. On the one hand, the gap configuration is shown in Fig. 5(a), where the distance d' between two vertices A_1 and A_2 is greater than zero, but the value of reaction force rf is zero. On the other hand, the contact configuration can be seen in Fig. 5(b), where the distance d' equals zero, but the value of reaction force rf can be greater than zero. This is summed up as:

$$\begin{cases} d' \geq 0 \\ rf \geq 0 \\ rf \cdot d' = 0 \end{cases} \tag{5}$$

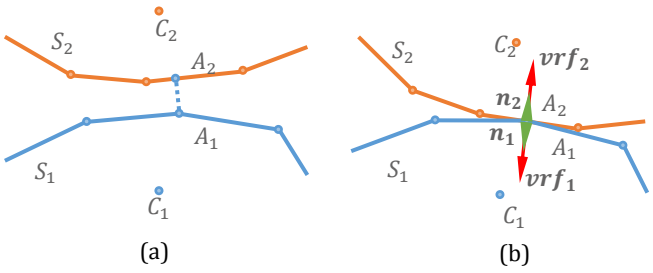

Fig. 5. Two configurations between surfaces: (a) gap (b) contact.

4.2. Formulation of the Problem

Based on the linearization of rigid body displacement and the concept of LCC, the relative positioning problem is transformed into an optimization problem. The formulation is shown in Equation (6). The objective function is the value of LCC ($rf \cdot d'$). The variables are displacements of skin model shapes, and the interaction forces between them. Reaction forces are constrained to be positive in the case of constraint (6a). Non-penetration constraints are expressed in constraint (6b). Constraints (6c) and (6d) correspond to the force balance and moment balance respectively.

$$\begin{aligned} find \quad & \boldsymbol{X} = \begin{bmatrix} \boldsymbol{SDTs} \\ \boldsymbol{rf} \end{bmatrix} \\ min \quad & rf \cdot d' = \left(\tfrac{1}{2}\boldsymbol{X}^T \begin{bmatrix} \boldsymbol{0} & \boldsymbol{A}^T \\ \boldsymbol{A} & \boldsymbol{0} \end{bmatrix} \boldsymbol{X} + [\boldsymbol{0} \quad \boldsymbol{d}^T]\boldsymbol{X}\right) \\ s.t. \quad & \begin{cases} (a)\ \boldsymbol{rf} \geq 0 \\ (b)\ \boldsymbol{A} \cdot \boldsymbol{SDTs} + \boldsymbol{d} \geq 0 \\ (c)\ \sum rf_{i,j} \cdot \boldsymbol{n_{i,j}} + \sum f_{i,k} \cdot \boldsymbol{n_{i,k}} = \boldsymbol{0} \\ (c)\ \sum \boldsymbol{L_{i,j}} \times \left(rf_{i,j} \cdot \boldsymbol{n_{i,j}}\right) + \\ \quad \sum \boldsymbol{L_{i,j}} \times \left(f_{i,k} \cdot \boldsymbol{n_{i,k}}\right) + \sum tq_{i,q} \cdot \boldsymbol{n_{i,q}} = \boldsymbol{0} \end{cases} \end{aligned} \tag{6}$$

This optimization is conducted iteratively to get the assembly result. The problem is solved using quadratic programming algorithms.

5. Comparison of Methods

The principles of the DM and LCC methods are different. However, both rely on solving an optimization problem. We could therefore compare these two methods from the point of view of optimization formulation. The comparison characteristics for both methods are shown in Table 1.

Based on the analysis of the assembly problem, both of the methods could translate DOF constraints to linear constraints equivalently. Meanwhile, geometry conditions, like non-penetration between mating surfaces, hold for both methods. They are transformed to linear constraints in the same way.

In the DM method, the load conditions (force and torque) are simplified and translated to the optimization objective equivalently. Based on Poinsot's theorem from screw theory, this translation is simple and reliable. In the LCC method, the load conditions are introduced to the constraints for system equilibrium.

In the DM method, the system equilibrium is a criterion which is used to select feasible assembly configurations from various simulation results. However, in the LCC method, the

system equilibrium is expressed explicitly as the optimization constraints. In the DM method, the interaction forces between parts are calculated only in the selection process. In the LCC method, the interaction force links the constraint to the objective.

Based on the analysis above, we can see that the LCC method uses more complex optimization objectives and constraints than the DM method. When the assembly is complex or the mesh quantity is large, solving LCC problems may require even more calculation than the DM method. Moreover, the LCC method requires quadratic programming algorithms, while the DM method can use linear programming algorithms.

Table 1. Comparison of simulation methods from optimization point of view.

Characteristic	DM Method	LCC Method
DOFs	Constraint	Constraint
Geometry Condition (Non-Penetration)	Constraint	Constraint
Load Condition	Objective (Direction) & Result Selection	Constraint
Interaction Force	Result Selection	Objective & Constraint
System Equilibrium	Result Selection	Constraint
Solver	Linear Programming	Quadratic Programming

6. Comparison of Assembly Examples

In this section, the simulation results of the proposed methods are compared. The skin model shapes are generated using the method in [19]. The assembly simulation methods were implemented under Matlab® environment, and the interior point algorithm was used to conduct optimization.

6.1. Mating of Two Surfaces

The first example is the mating of two square surfaces, which is shown in Fig. 6. The initial positions of surface $S1$ and $S2$ are shown in Fig. 6(a). As can be seen from the figure, form defects on these two surfaces are amplified. This makes it easier to verify the correctness of simulation results.

In the mating of surfaces, the displacements of $S1$ are constrained. Due to the assembly force, surface $S2$ will move towards $S1$. The translation of $S2$ along directions x and y and the rotation around direction z are constrained.

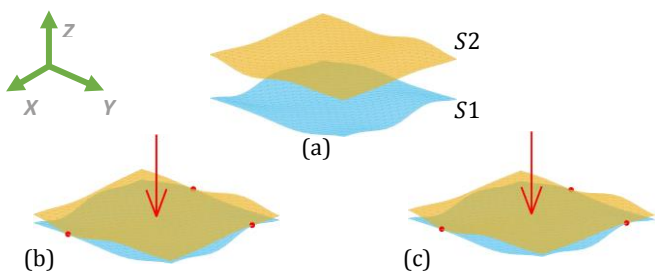

Fig. 6. Example of mating two surfaces: (a) initial position of two surfaces (b) mating result with LCC (c) mating result with DM.

Fig. 6(b) and (c) shows the mating result using the LCC method and the DM method respectively. The red arrows applied to $S2$ indicate the position and direction of the assembly force. Red points on the surfaces indicate the contact regions. It can be seen that the two methods generate consistent and identical results.

The coordinates of contact points in the simulation are listed in Table 2. Negligible differences are observed between the two simulation results.

Table 2 Contact point coordinates and the distance between them.

Method	Contact Point Coord. [mm]	Contact Distance [mm]
LCC	[1.00,0.25,0.03]	36×10^{-9}
	[0.50,-1,0.06]	50×10^{-9}
	[-1,0.5,0.05]	13×10^{-9}
MD	[1.01,0.26,0.03]	8×10^{-9}
	[0.51,-0.99,0.06]	30×10^{-9}
	[-0.99,0.51,0.05]	3×10^{-9}

6.2. Positioning of a Cube Part

The positioning of complex parts is a combination of several surface mating problems. The problem of positioning a cube part is shown in Fig. 7.

In Fig. 7(a), three forces in different directions are applied to the cube part. The size of the red arrows reflects the force value. In the DM method, these three forces are reduced to only one force, applying Poinsot's theorem.

There are three contact surfaces between the two parts. The contact position cannot be determined due to the influence of assembly forces. Fig. 7(b) shows the gaps between parts at initial positions.

Fig. 7(c) and 7(d) shows the position results of the LCC method and the DM method. Under the effect of form defects and assembly loads, the contact regions between parts are identical.

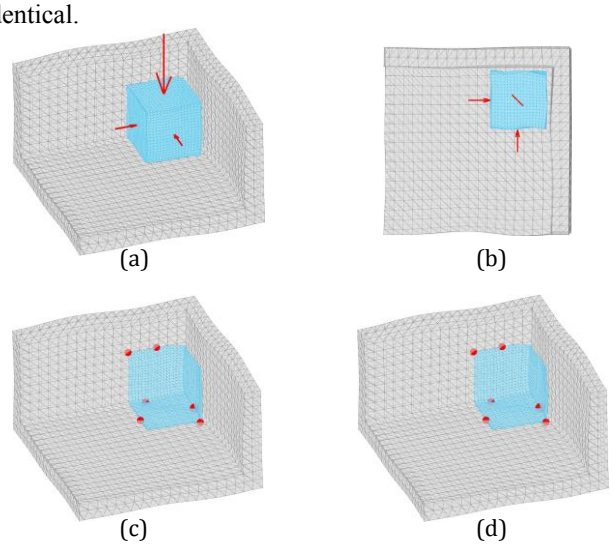

Fig. 7. Positioning of a cube part under assembly forces
(a, b) initial positions of parts, red arrows indicate assembly forces
(c) positioning result of LCC method (d) positioning result of DM method.

6.3. Assembly of 3 Parts

The assembly of 3 parts is shown in Fig. 8(a). Assembly forces are applied to parts. For the LCC method, these forces

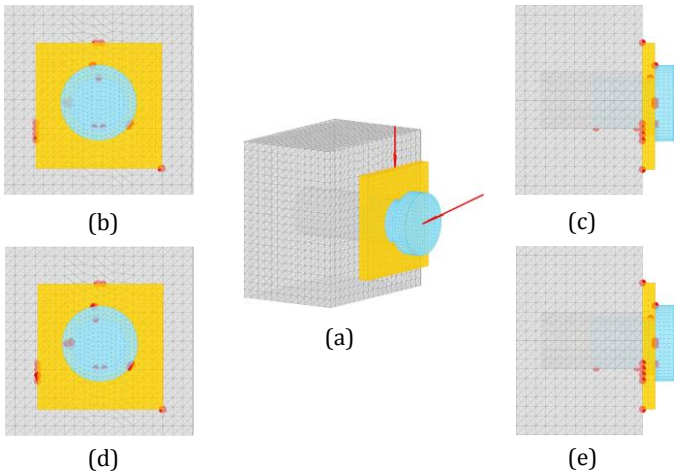

Fig. 8. Assembly of 3 parts (a) initial positions and assembly loads (b, c) assembly result of LCC method (d, e) assembly result of DM method.

are considered simultaneously, and the result is shown in Fig. 8(b) and 8(c). For the DM method, due to the multiple assembly parts and loads, two optimization sequences are considered. After checking the system balance, only one assembly result satisfies our requirements. This result is shown in Fig. 8(d) and 8(e).

6.4. Calculation Time and Precision

The calculation times are:

- example 1: DM and LCC: 3s
- example 2: DM and LCC: 8s
- example 3: DM: 15s; LCC: 37s.

With more complex models, the DM method is more efficient than the LCC method.

For the three examples, the two assembly simulation methods generate similar results. For all three examples and the two methods, the distances at the mating points are less than 16×10^{-9}mm. Errors are small enough to validate the two methods.

7. Conclusion

This work focuses on the assembly simulation using skin model shapes. First, the important characteristics for assembly simulation were analyzed. Based on the analysis, two simulation methods were proposed. The principles of the two methods were compared, and assembly examples were used to validate their effectiveness.

In future work, the two simulation methods will be compared considering algorithm precision and time efficiency on “real” mechanical products with many parts. Furthermore, part deformations caused by assembly loads can be introduced to generate more realistic results.

Acknowledgements

The authors would like to thank the China Scholarship Council (CSC) for the research funding.

References

[1] Requicha AAG. Toward a Theory of Geometric Tolerancing. Int J Robot Res 1983;2:45–60. doi:10.1177/027836498300200403.

[2] Desrochers A, Clément A. A dimensioning and tolerancing assistance model for CAD/CAM systems. Int J Adv Manuf Technol 1994;9:352–361.

[3] Bourdet P, Clément A. Controlling a complex surface with a 3 axis measuring machine. Ann CIRP 1976;25:359–361.

[4] Gao J, Chase KW, Magleby SP. Generalized 3-D tolerance analysis of mechanical assemblies with small kinematic adjustments. IIE Trans 1998;30:367–377.

[5] Desrochers A, Ghie W, Laperrière L. Application of a Unified Jacobian Torsor Model for Tolerance Analysis. J Comput Inf Sci Eng 2003;3:2. doi:10.1115/1.1573235.

[6] Teissandier D, Couetard Y, Gérard A. A computer aided tolerancing model: proportioned assembly clearance volume. Comput-Aided Des 1999;31:805–817.

[7] Davidson JK, Mujezinović A, Shah JJ. A New Mathematical Model for Geometric Tolerances as Applied to Round Faces. J Mech Des 2002;124:609. doi:10.1115/1.1497362.

[8] Ballu A, Mathieu L. Analysis of dimensional and geometrical specifications: standards and models. Proc. 3rd CIRP Semin. Comput. Aided Toler. Cachan Fr., 1993.

[9] Zhang M. Discrete shape modeling for geometrical product specification: contributions and applications to skin model simulation. École normale supérieure de Cachan-ENS Cachan, 2011.

[10] Samper S, Adragna P-A, Favreliere H, Pillet M. Modeling of 2D and 3D Assemblies Taking Into Account Form Errors of Plane Surfaces. J Comput Inf Sci Eng 2009;9:041005. doi:10.1115/1.3249575.

[11] Schleich B, Wartzack S. Approaches for the assembly simulation of skin model shapes. Comput-Aided Des 2015;65:18–33. doi:10.1016/j.cad.2015.03.004.

[12] Corrado A, Polini W, Moroni G, Petrò S. 3D Tolerance Analysis with Manufacturing Signature and Operating Conditions. Procedia CIRP 2016;43:130–5. doi:10.1016/j.procir.2016.02.097.

[13] Liu T, Cao Y, Wang J, Yang J. Assembly Error Calculation with Consideration of Part Deformation. Procedia CIRP 2016;43:58–63. doi:10.1016/j.procir.2016.02.007.

[14] Homri L, Goka E, Levasseur G, Dantan J-Y. Tolerance analysis -- Form defects modeling and simulation by modal decomposition and optimization. Comput-Aided Des 2017;91:46–59. doi:10.1016/j.cad.2017.04.007.

[15] Bourdet P, Mathieu L, Lartigue C, Ballu A. The concept of the small displacement torsor in metrology. Ser Adv Math Appl Sci 1996;40:110–122.

[16] Ledoux Y, Samper S, Grandjean J. Integrating form defects of mechanical joints into the tolerance studies. Adv. Math. Comput. Sci. Their Appl., Venice, Italy: WSEAS Press; 2016.

[17] Dai J. Screw algebra and kinematic approaches for mechanisms and robotics. Springer, London; 2014.

[18] Banerjee A, Chanda A, Das R. Historical Origin and Recent Development on Normal Directional Impact Models for Rigid Body Contact Simulation: A Critical Review. Arch Comput Methods Eng 2016. doi:10.1007/s11831-016-9164-5.

[19] Xingyu Yan, Alex Ballu. Generation of consistent skin model shape based on FEA method. Int J Adv Manuf Technol 2017. doi:10.1007/s00170-017-0177-5.